SCIENCE CHINA
Physics, Mechanics & Astronomy

• Article •

December 2014 Vol. 57 No. 12: 2276–2284
doi: 10.1007/s11433-014-5580-4

# Generating large steady-state optomechanical entanglement by the action of Casimir force

NIE WenJie[1,2,3*], LAN YueHeng[1], LI Yong[2*] & ZHU ShiYao[2]

[1]*Department of Physics, Tsinghua University, Beijing 100084, China;*
[2]*Beijing Computational Science Research Center, Beijing 100084, China;*
[3]*Department of Applied Physics East China Jiaotong University, Nanchang 330013, China*

Received May 7, 2014; accepted July 14, 2014; published online August 18, 2014

In this paper, we study an optomechanical device consisting of a Fabry-Pérot cavity with two dielectric nanospheres trapped near the cavity mirrors by an external driving laser. In the condition where the distances between the nanospheres and cavity mirrors are small enough, the Casimir force helps the optomechanical coupling to induce a steady-state optomechanical entanglement of the mechanical and optical modes in a certain regime of parameters. We investigate in detail the dependence of the steady-state optomechanical entanglement on external control parameters of the system, i.e., the effective detuning, the pump powers of the cavity, the cavity decay rate and the wavelength of the driving field. It is found that the large steady-state optomechanical entanglement, i.e. $E_N = 5.76$, can be generated with experimentally feasible parameters, i.e. the pump power $P = 18.2$ μW, the cavity decay rate $\kappa = 0.5$ MHz and the wavelength of the laser $\lambda_L$=1064 nm, which should be checked by optical measurement.

**optomechanics, Casimir effect, entanglement**

**PACS number(s):** 37.30.+i, 42.50.Wk, 42.50.Pq, 42.50.Lc

**Citation:** Nie W J, Lan Y H, Li Y, et al. Generating large steady-state optomechanical entanglement by the action of Casimir force. Sci China-Phys Mech Astron, 2014, 57: 2276–2284, doi: 10.1007/s11433-014-5580-4

The investigation of interaciton between micro-/nano-scaled mechanical oscillators and cavity fields is becoming an important subject in both theory and experiment for the control of mechanical motion at quantum level [1–5]. In such optomechanical systems the coupling between the mechanical and cavity modes increases enormously when the cavity field is driven with a strong pump laser, which enables an interesting demonstration of macroscopic quantum phenomena.

These optomechanical systems have been realized in a variety of physical setups, such as a Fabry-Pérot cavity with a movable end mirror [6–9], one or multi-membranes inside a standard Fabry-Pérot cavity [10–15], ultracold atomic ensembles or Kerr media in an optical cavity [16–20], a whispering-gallery cavity system [21–23] and a microresonator in a microwave transmission line resonator [24,25]. Several typical quantum-mechanical phenomena of macroscopic scale, such as, ground-state cooling of mechanical modes [6,7,26–29], quantum entanglement between optical and mechanical modes [8,30–35] or different mechanical modes [11,36–38], normal mode splitting in the displacement spectrum of mechanical oscillators [39], squeezed states of mechanical or optical modes [31,40,41] are investigated in detail in these ioptomechanical systems. In experiments, quantum regime of a mechanical oscillator has been reached with cavity cooling [42,43]. In addition, the optical bistability and optomechanically induced transparency are also discussed in optomechanical systems [21,44–49]. The optomechanical systems have many potential applications, i.e., measurement of small displacement and force [50], detection of gravitational waves [51] and quantum communication and information processing [52,53].

In general, the movable part such as a mechanical oscilla-

*Corresponding author (NIE WenJie, email: henameiswen@sina.com; LI Yong, email: liyong@csrc.ac.cn)

tor in an optomechanical system needs to be supported by a cantilever and therefore the influence of thermal fluctuations in the environment is unavoidable. Thus quantum characteristics of the mechanical oscillator are not stable and hence thermal noise should be suppressed by pre-cooling the system down to low temperature cryogenically. In contrast to the optomechanical setup with direct coupling between the mechanical oscillator and the thermal lead, the optomechanical system with a levitated mirror or trapped dielectric nanosphere is able to inherently manifest the quantum features of a mechanical system and has aroused a lot of interest recently [54–67]. In this kind of optomechanical systems, the levitated scatterer is trapped inside a high-vacuum chamber optically by the driving laser and consequently the influence of the thermal noise is significantly reduced due to the absence of the mechanical contact. A series of applications of the optomechanical system are proposed, e.g., measurement of the gravitational waves [57], of non-Newtonian force, of Casimir force [62,68], and of single molecules collisions [69]. In the quantum regime of the system, the quantum mechanically entangled and squeezed states and macroscopic quantum superposition states are expected to be seen [55,70,71].

In this work, we consider an optomechanical system consisting of a Fabry-Pérot cavity and two dielectric nanospheres trapped near the surfaces of cavity mirrors by external driving laser. When the separation between the nanosphere and the cavity mirror surface is of the order of nanometers, the motion of each dielectric nanosphere is forced by the optical radiation pressure and the Casimir interaction. In this case, the nonzero effective optomechanical coupling appears due to the Casimir force biasing the original steady-state position. It is also noted that the present model only has a cavity field and therefore is different from the previous scheme in reference [38], where the nonzero effective optomechanical coupling between the trapped particles and optical mode is generated by trapping the particles in a ring cavity with two degenerate counter-propagating cavity modes. The nonzero effective optomechanical couplings are the basis of the steady-state optomechanical entanglement between the mechanical and optical modes. We investigate the steady-state optomechanical entanglement between the dielectric nanospheres and the cavity mode with the help of Heisenberg equations of motion. The generated steady-state entanglement can be relatively large with proper system parameters and is related directly to the Casimir interaction. Further, we also discuss in detail the influence of the pump power, the cavity decay rate and the wavelength of the driving laser on the steady-state entanglement. In particular, we find that the steady-state entanglement between the two nanospheres does not appear in the present model.

## 1 The model system and the equation of motion

The optomechanical system investigated here is depicted in Figure 1, where two dielectric nanospheres with radius $r_1$ and $r_2$ are optically levitated in a Fabry-Pérot cavity by a driving laser with power $P$. The driven cavity mode interacts with these nanospheres and therefore is responsible for their trapping and cooling. In particular, we assume that the dielectric nanosphere $r_1$ ($r_2$) is trapped near the antinode of the driven cavity field closest to the surface of the first (second) cavity mirror. In this case, the motion of the levitated nanospheres' center-of-mass (c.m.) is driven not only by the optical radiation pressure but also by the Casimir force between the trapped nanospheres and the cavity mirrors, which arises from the zero-point energy fluctuation of vacuum [72–74]. The action of the Casimir force on the dielectric nanosphere also leads to nonzero effective optomechanical coupling between the nanosphere and the cavity field [63,64]. Consequently, the steady-state optomechanical entanglement between the nanospheres and the driven cavity mode is achieved. Here we investigate in detail the steady-state optomechanical entanglement between each levitated nanosphere and the cavity field with the help of Heisenberg equation of motion, which can be made relatively strong with proper selection of Casimir coupling strength and other external control parameters of the system.

The Hamiltonian of the proposed optomechanical system in the rotating frame of the laser field with frequency $\omega_L$ is given by [54,55]

$$\begin{aligned} H &= \hbar\Delta_0 a^\dagger a + \frac{p_1^2}{2m_1} + \frac{p_2^2}{2m_2} - \hbar g_1 a^\dagger a \cos^2(kx_1) \\ &\quad -\hbar g_2 a^\dagger a \cos^2(kx_2) - \frac{\eta\hbar\pi^3 c r_1}{720(d-r_1-x_1)^2} \\ &\quad -\frac{\eta\hbar\pi^3 c r_2}{720(d-r_2-x_2)^2} + \mathrm{i}\hbar(\varepsilon_0 a^\dagger - \mathrm{H.c.}), \end{aligned} \tag{1}$$

where $\Delta_0 = \omega_C - \omega_L$, is the detuning between the driving field of frequency $\omega_L$ and the corresponding cavity mode of frequency $\omega_C = kc$, ($c$ is the speed of light in vacuum). The photon annihilation operator in the cavity mode, $a$, satisfies

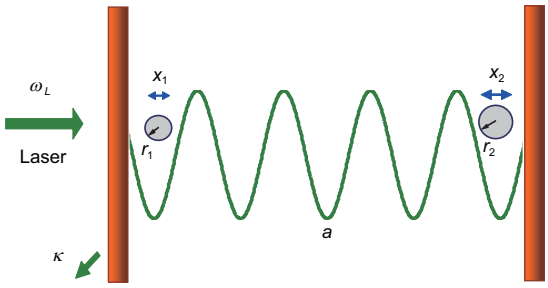


**Figure 1** (Color online) An optomechanical system with two levitated dielectric nanospheres. The two dielectric nanospheres are trapped and cooled near the antinodes closest to left and right cavity mirrors, by an external pump laser. The motion of each levitated nanosphere is forced by the optical radiation pressure and Casimir interaction arising from the zero-point fluctuation of the electromagnetic field in the vacuum.

the commutation relation $[a, a^{\dagger}] = 1$. $m_1$ and $m_2$ are the masses of the left and right dielectric nanospheres, respectively; $x_1$ ($x_2$) and $p_1$ ($p_2$) are the position and momentum operators for the c.m. of the left (right) nanosphere with commutation relation $[x_j, p_j] = \mathrm{i}\hbar$ ($j = 1, 2$); $g_1 = \dfrac{3V_1}{4V_c}\dfrac{\epsilon-1}{\epsilon+2}\omega_C$ and $g_2 = \dfrac{3V_2}{4V_c}\dfrac{\epsilon-1}{\epsilon+2}\omega_C$ are the corresponding coupling strengths, where $V_1$ ($V_2$) is the volume of the left (right) nanosphere, $V_c$ is the optical mode volume and $\epsilon$ is the dielectric constant of the nanospheres. The sixth and seventh terms on the right side of eq. (1) denote the Casimir energies between the nanospheres and the corresponding cavity mirrors, which depend strongly on the separation between them [75–77]. However, under the proximity force approximation in the limit of small distance $d - r_j \ll r_j$ [73], the Casimir force can be simplified as $F_{Cj} = -\eta\dfrac{\hbar\pi^3 c r_j}{360\left(d-r_j\right)^3}$, and the corresponding Casimir energy is $E_{Cj} = -\dfrac{\eta\hbar\pi^3 c r_j}{720(d-r_j)^2}$, where $d = \lambda/4$ ( $\lambda = 2\pi/k$ is the wavelength of the cavity field). The prefactor $\eta$ is included for characterizing the reduction in the Casimir energy or force compared to that between two perfect conductors [75,76,78], and has been assumed to be the same for the left and right dielectric nanosphere. The simplified result is expected to be valid for $d - r_j < r_j$ [78]. It is noted that the correction to the Casimir potential energy due to the motion of the nanosphere is neglected because the dynamic correction is small and therefore plays a secondary role in studying the optomechanical entanglement due to the action of the Casimir force [79]. The last term in eq. (1) describes the interaction of the cavity mode with the pump laser of amplitude $|\varepsilon_0| = \sqrt{2P\kappa/\hbar\omega_L}$, where $\kappa$ is the decay rate of the cavity. In addition, we assume that the driving field is not so strong as to melt the nanosphere.

Based on the Hamiltonian of the optomechanical system, we can investigate in detail its quantum dynamics with the Heisenberg-Langevin formalism. The full dynamics of the system should also include the fluctuation-dissipation processes affecting the optical field and the levitated dielectric nanospheres. However, in order to levitate the nanosphere robustly, the optomechanical device should be placed in a sufficiently high vacuum chamber. Consequently, a high mechanical quality factor is attained for the optically trapped nanosphere, in which case the noise force acting on the nanosphere can be neglected [56]. By using the Hamiltonian (1) and taking into account quantum fluctuation of the optical field, the Heisenberg-Langevin equations describing the dynamics of the system can be written as:

$$\dot{x}_1 = p_1/m_1, \tag{2}$$

$$\dot{p}_1 = -\hbar g_1 k a^{\dagger} a \sin(2kx_1) + \frac{\eta\hbar\pi^3 c r_1/360}{(d-r_1-x_1)^3}, \tag{3}$$

$$\dot{x}_2 = p_2/m_2, \tag{4}$$

$$\dot{p}_2 = -\hbar g_2 k a^{\dagger} a \sin(2kx_2) + \frac{\eta\hbar\pi^3 c r_2/360}{(d-r_2-x_2)^3}, \tag{5}$$

$$\dot{a} = -\mathrm{i}\Delta_0 a + \mathrm{i}g_1\cos^2(kx_1)a + \mathrm{i}g_2\cos^2(kx_2)a - \kappa a + \varepsilon_0 + \sqrt{2\kappa}a_{in}, \tag{6}$$

where the overdots denote time derivatives. $a_{in}$ is the cavity-field quantum vacuum fluctuation, which is fully characterized by the correlation $\langle a_{in}(t)\, a_{in}^{\dagger}(t')\rangle = \delta(t-t')$ in the Markovian approximation. In order to investigate the optomechanical entanglement between the optical and mechanical modes, we should choose a proper steady-state operating point where the effective couplings between the cavity field and two nanospheres are large due to the intensely driven cavity field. The steady-state values sensitively depend on the strength of the Casimir interaction between the levitated nanosphere and the cavity mirror.

When deriving the steady-state values, we take first-order approximation for the optomechanical and Casimir interactions because the positive steady-state positions $x_{js}$, are very small compared to the distance $d - r_j$ [55], that is, $0 < x_{js}/(d-r_j) \ll 1$. Under these approximations, the constant steady-state expectation values of the nanosphere position and cavity field strength can be obtained analytically by factorizing eqs. (2)–(6) and setting the time derivatives to zero as:

$$p_{1s} = 0,\ p_{2s} = 0, \tag{7}$$

$$x_{js} = \frac{\eta\pi^3 c r_j\left(d-r_j\right)}{720 g_j k^2|\alpha_s|^2\left(d-r_j\right)^4 - 3\eta\pi^3 c r_j}, \tag{8}$$

$$\alpha_s = \frac{\varepsilon_0}{\kappa + \mathrm{i}\Delta}, \tag{9}$$

where $\Delta = \Delta_0 - g_1\cos^2(kx_{1s}) - g_2\cos^2(kx_{2s})$ is the effective detuning of the cavity mode. It is obvious that the Casimir interaction influences strongly the steady-state values of the system and in the absence of Casimir force, the steady-state positions always equal zero, that is, $x_{1s} = x_{1s} = 0$, which represent origins of our position coordinates. Further, by using eqs. (8) and (9) and the condition $0 < x_{js}/(d-r_j) \ll 1$, we can infer that the effective detuning of the optomechanical system should satisfy $|\Delta| \ll \sqrt{\dfrac{180\varepsilon_0^2(d-r_j)^4 g_j k^2}{\eta\pi^3 c r_j} - \kappa^2}$. This also means that we should select proper system parameters, i.e., the pump power, the radii of the nanospheres and the cavity decay rate, since the effective detuning $\Delta$ is a real number.

## 2 Dynamics of the quantum fluctuations

In general an optomechanical system is always subject to the action of optical loss and random noise. Therefore, we need to investigate fluctuations in positions and momenta of the mechanical oscillators and of the intracavity field, and quantum correlation between them, which are seen to induce a stationary and robust optomechanical entanglement between the optical and mechanical modes. In the following, we focus on

the dynamics of quantum fluctuations around the steady state under linear approximation.

The operators in eqs. (2)–(6) can be splitted into their steady-state expectation values and the corresponding quantum fluctuations, e.g., $x_j = x_{js} + \delta x_j$, $p_j = p_{js} + \delta p_j$ and $a = \alpha_s + \delta a$. Explicitly, substituting these expressions into eqs. (2)–(6), we obtain a set of linearized equations of motion for the fluctuation operators,

$$\delta\dot{x}_1 = \omega_1 \delta p_1, \tag{10}$$

$$\delta\dot{p}_1 = -\omega_1 \delta x_1 - G_1(\alpha_s^* \delta a + \alpha_s \delta a^\dagger), \tag{11}$$

$$\delta\dot{x}_2 = \omega_2 \delta p_2, \tag{12}$$

$$\delta\dot{p}_2 = -\omega_2 \delta x_2 - G_2(\alpha_s^* \delta a + \alpha_s \delta a^\dagger), \tag{13}$$

$$\delta\dot{a} = -(\kappa + \mathrm{i}\Delta)\delta a - \mathrm{i}G_1\alpha_s \delta x_1 - \mathrm{i}G_2\alpha_s \delta x_2 + \sqrt{2\kappa}\hat{a}_{in}, \tag{14}$$

where $G_j = g_j k \sin(2kx_{js})/\sqrt{m_j\omega_j/\hbar}$. The position and momentum fluctuations $\delta x_j$ and $\delta p_j$ have been nondimensionalized as $\sqrt{\frac{m_j\omega_j}{\hbar}}\delta x_j \to \delta x_j$ and $\sqrt{\frac{1}{\hbar m_j\omega_j}}\delta p_j \to \delta p_j$ in eqs. (10)–(14). It is also noted that $\omega_1\,(\omega_2\,)$ is the frequency associated with the center-of-mass oscillation of the left (right) dielectric nanosphere, which is determined by the driving optical field and the Casimir interactions, e.g., $\omega_j = \sqrt{\frac{2\hbar g_j k^2|\alpha_s|^2}{m_j}\cos(2kx_{js}) - \frac{\eta\hbar\pi^3 c r_j}{120 m_j (d - r_j - x_{js})^4}}$. The effective frequency is always larger than zero, i.e., $\omega_j > 0$, as the effective detuning $|\Delta| \ll \sqrt{\frac{180\varepsilon_0^2 (d - r_j)^4 g_j k^2}{\eta\pi^3 c r_j} - \kappa^2}$. In eqs. (10)–(14), we neglect all the terms higher than linear order in the fluctuations $\delta x_j$, $\delta p_j$ and $\delta a$ because the photon numbers in the cavity is so large that the condition $|\alpha_s| \gg 1$ can be always satisfied.

It is convenient to rewrite the linearized dynamics of the system by introducing the field quadrature fluctuation operators, $\delta X = \left(\delta a + \delta a^\dagger\right)/\sqrt{2}, \delta Y = \left(\delta a - \delta a^\dagger\right)/\sqrt{2}\mathrm{i}$, and the corresponding Hermitian input noise operators $X_{in} = \left(\delta a_{in} + \delta a_{in}^\dagger\right)/\sqrt{2}, Y_{in} = \left(\delta a_{in} - \delta a_{in}^\dagger\right)/\sqrt{2}\mathrm{i}$,

$$\delta\dot{x}_1 = \omega_1 \delta p_1, \tag{15}$$

$$\delta\dot{p}_1 = -\omega_1 \delta x_1 - G_{1X}\delta X - G_{1Y}\delta Y, \tag{16}$$

$$\delta\dot{x}_2 = \omega_2 \delta p_2, \tag{17}$$

$$\delta\dot{p}_2 = -\omega_2 \delta x_2 - G_{2X}\delta X - G_{2Y}\delta Y, \tag{18}$$

$$\delta\dot{X} = G_{1Y}\delta x_1 + G_{2Y}\delta x_2 - \kappa\delta X + \Delta\delta Y + \sqrt{2\kappa}X_{in}, \tag{19}$$

$$\delta\dot{Y} = -G_{1X}\delta x_1 - G_{2X}\delta x_2 - \Delta\delta X - -\kappa\delta Y + \sqrt{2\kappa}X_{in}, \tag{20}$$

where $G_{jX} = G_j(\alpha_s^* + \alpha_s)/\sqrt{2}$ and $G_{jY} = \mathrm{i}G_j(\alpha_s^* - \alpha_s)/\sqrt{2}$. In general, the values of $G_{1Y}$ and $G_{2Y}$ can be made zero by choosing a proper phase of the cavity field. Consequently, the effective optomechanical coupling between the mechanical and cavity modes are $G_{1X} = \sqrt{2}G_1|\alpha_s|$ and $G_{2X} = \sqrt{2}G_2|\alpha_s|$, which can be made very large by increasing the intracavity photon number and adjusting the strength of the Casimir interaction and therefore enable the optomechanical entanglement in a certain range of system parameters. Furthermore, by introducing the column vector of fluctuation operators $u^{\mathrm{T}}(t) = (\delta x_1(t), \delta p_1(t), \delta x_2(t), \delta p_2(t), \delta X(t), \delta Y(t))$ and the corresponding column vector of noises $n^{\mathrm{T}}(t) = (0, 0, 0, 0, \sqrt{2\kappa}X_{in}, \sqrt{2\kappa}Y_{in})$, eqs. (15)–(20) can be written in a compact matrix form:

$$\dot{u}(t) = Ju(t) + n(t), \tag{21}$$

where $J$ is the drift matrix

$$J = \begin{pmatrix} 0 & \omega_1 & 0 & 0 & 0 & 0 \\ -\omega_1 & 0 & 0 & 0 & -G_{1X} & -G_{1Y} \\ 0 & 0 & 0 & \omega_2 & 0 & 0 \\ 0 & 0 & -\omega_2 & 0 & -G_{2X} & -G_{2Y} \\ G_{1Y} & 0 & G_{2Y} & 0 & -\kappa & \Delta \\ -G_{1X} & 0 & -G_{2X} & 0 & -\Delta & -\kappa \end{pmatrix}. \tag{22}$$

The steady state of the system is unique when the solutions to eq. (21) are stable, which requires that the real parts of all the eigenvalues of the matrix $J$ are negative. The stability condition for the system can be obtained by using the Routh-Hurwitz criteria [80]. However, the explicit inequalities are not given here since they are quite cumbersome. We resort to numerical calculation to discuss steady-state solutions. Hereafter, the stability condition is always satisfied with our chosen system parameters.

## 3 Steady-state optomechanical entanglement

Since the quantum noises of cavity field are white and the dynamics of quantum fluctuations is linearized, the state of the system is a zero-mean Gaussian one which is fully determined by the $6 \times 6$ correlation matrix with the real matrix element $V_{ij} = \langle u_i(\infty)\, u_j(\infty) + u_j(\infty)\, u_i(\infty)\rangle/2$. The steady-state correlation matrix $V$ can be obtained by solving the linearized Langevin equation (21) for the quantum fluctuation, which satisfies the following Lyapunov equation [8]:

$$JV + VJ^{\mathrm{T}} = -D, \tag{23}$$

where $D$ =diag$[0, 0, 0, 0, \kappa, \kappa]$. Eq. (23) is linear and straightforwardly solved. In spite of this fact, the explicit solution is cumbersome and therefore not reported here. Instead, we solve the equation with numerical calculation and study the steady-state optomechanical entanglement between each nanosphere and the cavity field.

In order to check the generated optomechanical entanglement due to the action of the Casimir force, we consider the bipartite entanglement between a single mechanical and cavity mode, which is quantified using the logarithmic negativity $E_N$ and given by [8]

$$E_N = \max[0, -\ln 2\nu_{\min}], \tag{24}$$

where $\nu_{\min}$ is the smallest symplectic eigenvalue of the partially transposed $4 \times 4$ correlation matrix associated with the

selected bipartite subsystem, which can be obtained by neglecting the columns and rows of uninteresting modes in the original correlation matrix $V$. The reduced $4\times4$ correlation matrix can be written in a $2\times2$ block form as [8]:

$$V_{bp}=\begin{pmatrix}A & C\\ C^{\mathrm{T}} & B\end{pmatrix}. \tag{25}$$

In this manner, the smallest symplectic eigenvalue is $\nu_{\min}=2^{-1/2}\left[\Sigma-\left(\Sigma^2-4\det V_{bp}\right)^{1/2}\right]^{1/2}$ with $\Sigma=\det A+\det B-2\det C$.

In the following, we investigate the steady-state entanglements between the nanospheres and the cavity field, measured by the logarithmic negativity, $E_N^{(1)}$ and $E_N^{(2)}$. It is also noted that the steady-state entanglement between the two nanospheres can be calculated straightforwardly with eq. (24) and properly selected reduced correlation matrix. However, we find that the entanglement between them can not be generated for the present model and therefore we only focus on the optomechanical entanglement between the mechanical and optical modes in the following. It is stressed that the steady-state entanglement is generated by the effective optomechanical couplings $G_{1X}$ and $G_{2X}$ between the mechanical and cavity modes, which are related directly to the Casimir force and the optical radiation pressure. In particular, the effective optomechanical couplings are always zero in the absence of Casimir force. Consequently, the Casimir interaction plays a dominant role in producing the optomechanical entanglement.

Figure 2 shows the steady-state positions, $x_{1s}$ and $x_{2s}$, the effective frequencies, $\omega_1$ and $\omega_2$, and the effective optomechanical couplings, $G_{1X}$ and $G_{2X}$, as a function of the effective detuning $\Delta$, for the identical sphere size $r_1=r_2=160$ nm and $d-r_j=106$ nm with the wavelength of the laser $\lambda_L\approx\lambda=1064$ nm. The density and the dielectric constant of both nanospheres (silicon materials) are $\rho=2300$ kg/m$^3$ and $\epsilon=2$. Further, we consider the cavity mirrors with a thick dielectric (SiN) membrane coated with 200 nm of gold, and in this case the prefactor in the Casimir interaction $\eta\simeq0.13$ [62]. The optical cavity has a length $L=3$ mm and the pump power $P=20$ μW. The cavity decay rate, the mode waist and the corresponding mode volume are $\kappa=0.5$ MHz, $w=25$ μm, and $V_c=(\pi/4)Lw^2$.

It can be seen from Figure 2 that due to the reflection symmetry in the system, the steady-state position, $x_{1s}\equiv x_{2s}$, the effective frequency, $\omega_1\equiv\omega_2$ and the effective optomechanical coupling, $G_{1X}\equiv G_{2X}$. Further, with the above system parameters, the absolute value of the effective detuning $|\Delta|$ should satisfy $|\Delta|\ll\sqrt{\dfrac{180\varepsilon_0^2(d-r_j)^4g_jk^2}{\eta\pi^3cr_j}-\kappa^2}\approx1.21$ MHz, which corresponds to $x_{js}/(d-r_j)\ll1$. In this regime, the intracavity mean photon number is large and hence the system works in the region of single stability. It is seen from Figure 2(b) that the effective frequency of the nanospheres decreases with the increasing absolute value of the effective detuning and attains a maximum when the effective detuning $\Delta=0$. Correspondingly, we see from Figure 2(c) that the effective optomechanical coupling increases with the increasing magnitude of the effective detuning and attains a minimum at $\Delta=0$. The nonzero effective optomechanical coupling enables the large optomechanical entanglement between the optical and mechanical modes (see below).

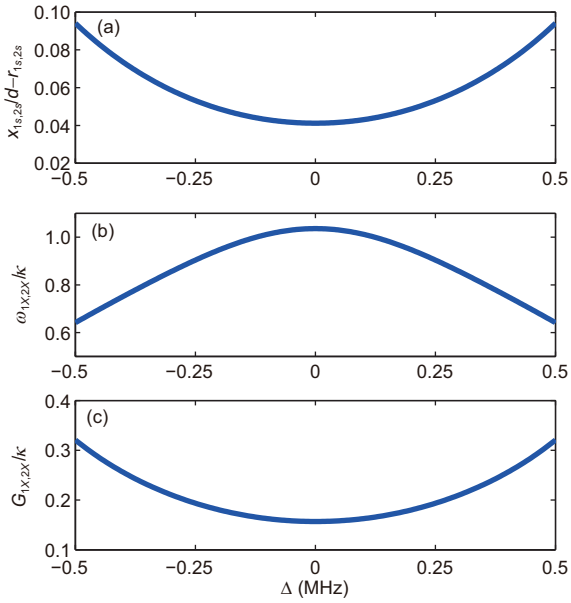


**Figure 2** (Color online) The steady-state positons, $x_{1s}=x_{2s}$, the effective optomechanical couplings, $G_{1X}=G_{2X}$, and the effective frequency, $\omega_1=\omega_2$, as a function of the effective detuning $\Delta$, for identical sphere size $r_1=r_2=160$ nm and $d-r_j=106$ nm with the wavelength of the laser $\lambda_L\approx\lambda=1064$ nm. The cavity decay rate, the mode waist and the corresponding mode volume are $\kappa=0.5$ MHz, $w=25$ μm, and $V_c=(\pi/4)Lw^2$; the density and dielectric constant of both nanospheres (silicon materials) are $\rho=2300$ kg/m$^3$ and $\epsilon=2$; the prefactor in the Casimir interaction $\eta\simeq0.13$; the optical cavity length $L=3$ mm and the pump power $P=20$ μW.

Figure 3 shows the bipartite entanglements $E_N^{(1)}$ and $E_N^{(2)}$ as a function of the effective detuning $\Delta$ with $r_1=150$ nm and several different radii of the right nanosphere. It is clear from Figure 3 that with the fixed radii of the nanospheres, the entanglement increases with increasing effective detuning and disappears suddenly at a special negative detuning. The maximum optomechanical entanglements appear near zero effective detuning for different radii of the nanospheres. The optimal results are different from the previous optomechanical system with a movable mirror, where the optimal entanglement appears in the regime $\Delta\approx\omega_m$ ($\omega_m$ is the frequency of the mechanical oscillator) corresponding to the optimal cooling of a mechanical oscillator [8]. This is due to that in the present optomechanical system, the thermal lead is removed by trapping optically the nanosphere and therefore the mechanical damping rates can be negligible. In addition, when the effective detuning approaches zero, the effective frequencies of the nanospheres can be larger than the cavity decay rate, i.e. $\omega_{1,2}/\kappa>1$ (see Figure 2), which is located at the resolved sideband region of the optomechanical system [28,29] and optimal optomechanical entanglement can be

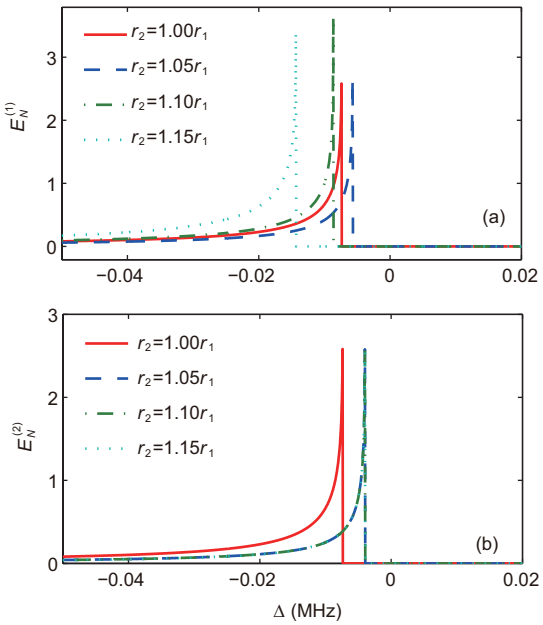


**Figure 3** (Color online) The logarithmic negativities, $E_N^{(1)}$ and $E_N^{(2)}$, as a function of the effective detuning Δ for different radii of the right nanosphere $r_2$ with fixed $r_1$ = 150 nm. For other parameters, see Figure 2.

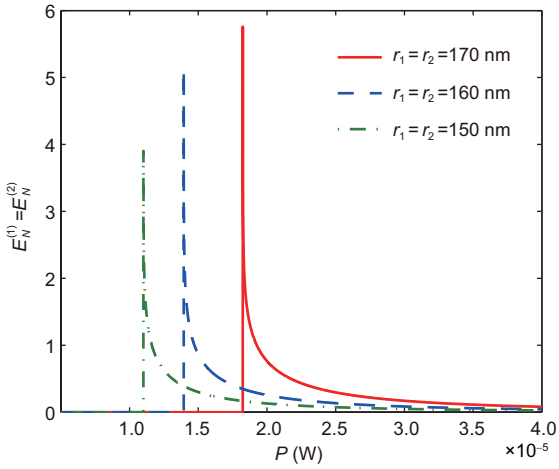


**Figure 4** (Color online) The logarithmic negativity, $E_N^{(1)}$ and $E_N^{(2)}$, as a function of the pump power $P$ near zero effective detuning, i.e. Δ = −0.03 MHz. Here the nanospheres are identical, which means $r_1 = r_2$, $E_N^{(1)} = E_N^{(2)}$. Other parameters are the same as in Figure 2.

obtained even with weak optomechanical couplings.

In addition, we see from Figure 3(a) that the logarithmic negativity $E_N^{(1)}$ increases with increasing radius of the right nanosphere, e.g., $r_2 = 1.15r_1$. In particular, the effective frequency of the left nanosphere $\omega_1$ and the optomechanical coupling $G_{1X}$ between the nanosphere and the optical field cannot be altered with increasing radius of the right nanosphere. This means that the optomechanical coupling between the right nanosphere and the cavity mirror also influences the steady-state entanglement between the optical field and the left nanosphere. It is observed from Figure 3(b) that when $r_2 > r_1$, the entanglement between the right nanosphere and the cavtiy mode is almost independent of its radius.

In Figure 4 we study the dependence of the optomechanical entanglements, $E_N^{(1)}$ and $E_N^{(2)}$, on the pump power $P$ near zero effective detuning, i.e. $\Delta = -0.03$ MHz with different radii of the nanospheres. It is noted that the selected range of the pump power satisfies the condition $|\Delta| \ll \sqrt{\frac{180\varepsilon_0^2(d-r_j)^4 g_j k^2}{\eta\pi^3 c r_j} - \kappa^2}$ when the effective detuning is fixed. We now assume that the two nanospheres are identical. Thus the entanglement $E_N^{(1)} = E_N^{(2)}$ due to the symmetry of the system.

We see from Figure 4 that the optomechanical entanglement always increases with decreasing pump power. In the symmetric case with the identical sphere size, both entanglements decrease with decreasing nanosphere size and Casimir interaction strength. Similarly, the entanglement disappears suddenly at a special pump power, which is different for different radii. We stress that the generated optomechanical entanglement by nonzero effective optomechanical couplings could be large with properly chosen system parameters. For example, $E_N^{(1)} = E_N^{(2)} = 5.76$ when $P = 18.2$ μW and $r_1 = r_2 = 170$ nm. This increases by an order-of-magnitude the optomechanical entanglement between the movable mirror and the cavity field [8] and therefore can be checked easily by optical measurement. The large optomechanical entanglement is similar to zero temperature entanglement [31] and is partially attributed to the negligible thermal noise of the system when the nanospheres are trapped optically inside a high vacuum chamber. In this case, the decay rate of the optical mode will be much larger than the damping rate of the mechanical mode and therefore the large entanglement can easily be attained [30]. We stress that in the present optomechanical model, spheres with nanometer size can be manufactured easily with current nanotechnology. Further, nanospheres can be trapped and levitated optically inside a Fabry-Pérot cavity by an external driving laser [58,65]. In particular, the selected system parameters of the optical cavity used for generating large steady-state optomechanical entanglement is universal and therefore experimentally feasible. With the homodyne detection, one can measure experimentally all independent entries of the correlation matrix $V_{bp}$, and therefore calculate the logarithmic negativity, which quantifies the degree of entanglement [8].

Figure 5 shows the dependence of the optomechanical entanglements, $E_N^{(1)}$ and $E_N^{(2)}$, on the cavity decay rate $\kappa$ near zero effective detuning, i.e. $\Delta = -0.03$ MHz with different radii of the nanosphere. It is obvious that the nonzero logarithmic negativity is an increasing function of the cavity decay rate $\kappa$ and hence the entanglement becomes stronger with larger values of $\kappa$. Further, the region for nonzero entanglement in the cavit decay rate $\kappa$ increases as the radii of both nanospheres decrease.

We then investigate the dependence of the optomechanical entanglement on the wavelength of the driven cavity field $\lambda$. Figure 6 shows the dependence of $E_N^{(1)}$ and $E_N^{(2)}$, on the wave-

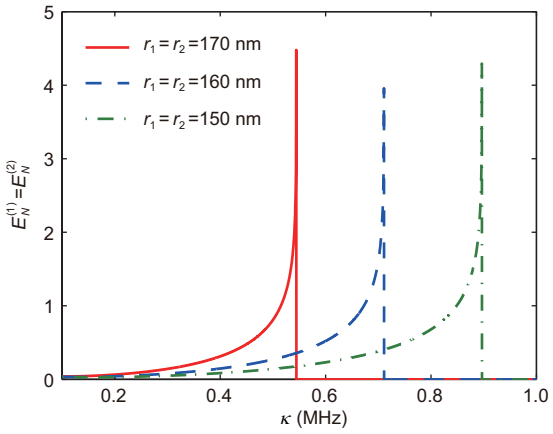


**Figure 5** (Color online) The logarithmic negativity, $E_N^{(1)}$ and $E_N^{(2)}$ ($E_N^{(1)} = E_N^{(2)}$ with identical sphere size $r_1 = r_2$), as a function of the cavity decay rate $\kappa$ near zero effective detuning, i.e. $\Delta = -0.03$ MHz. Other parameters are the same as in Figure 2.

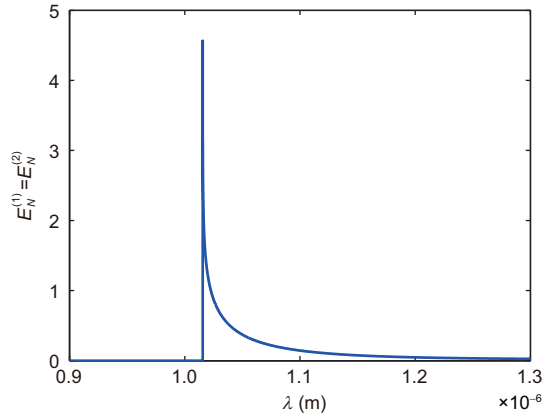


**Figure 6** (Color online) The logarithmic negativity, $E_N^{(1)}$ and $E_N^{(2)}$ ($E_N^{(1)} = E_N^{(2)}$ with identical sphere size $r_1 = r_2$), as a function of the wavelength of the driven cavity field $\lambda$ near zero effective detuning, i.e. $\Delta = -0.03$ MHz. Other parameters are the same as in Figure 2.

length $\lambda$ at given effective detuning $\Delta = -0.03$ MHz and $r_1 = r_2 = 160$ nm. It is obvious from Figure 6 that the entanglement increases with decreasing wavelength. When the radius of the nanosphere is fixed, the distance between the nanosphere and the cavity mirror decreases with decreasing wavelength $\lambda$. Consquently, the strength of the Casimir interaction increases and therefore the optomechanical entanglement rises. However, the optomechanical entanglement disappears with very small wavelength. In order to achieve large optomechanical entanglement, we should select proper wavelength for the driving field.

## 4 Conclusions

In conclusion, we investigate the steady-state optomechanical entanglement in an optomechanical system consisting of two dielectric nanospheres and a Fabry-Pérot cavity driven by a single-mode optical field. The dielectric nanospheres are trapped and levitated near the left and right cavity mirrors, respectively. In this case, the center-of-mass (c.m.) motion of the levitated nanospheres is driven by both the optical radiation pressure and the Casimir force between the trapped nanosphere and the cavity mirror. Correspondingly, the steady-state positions of the dielectric nanospheres depend strongly on the Casimir interaction, which induces a nonzero effective optomechanical coupling between the nanosphere and the cavity field in the linear approximation. Further, we investigated in detail the optomechanical entanglement induced by the nonzero effective optomechanical coupling due to the Casimir interaction, measured by the logarithmic negativity $E_N$, as a function of various parameters of the system with linearized dynamics around semiclassical steady-states. We showed that a relatively large optomechanical entanglement between the mechanical and optical modes, i.e. $E_N$=5.76, can be generated with experimentally feasible parameters for the present optomechanical system, i.e. the pump power $P = 18.2$ μW, the cavity decay rate $\kappa = 0.5$ MHz and the wavelength of the laser $\lambda_L$=1064 nm. The results obtained here are useful for quantum control of mechanical devices and measurement of optomechanical entanglement.

*This work was supported by the National Basic Research Program of China (Grant Nos. 2011CB922203, 2012CB921603 and 2012CB922104) and the National Natural Science Foundation of China (Grant Nos. 11304010, 11174027 and 11375093).*

1 Kippenberg T J, Vahala K J. Cavity opto-mechanics. Opt Express, 2007, 15: 17172–17205
2 Kippenberg T J, Vahala K J. Cavity optomechanics: Back-action at the mesoscale. Science, 2008, 321: 1172–1176
3 Marquardt F, Girvin S M. Trend: Optomechanics. Physics, 2009, 2: 40
4 Aspelmeyer M, Gröblacher S, Hammerer K, et al. Quantum optomechanics-throwing a glance [Invited]. J Opt Soc Am B, 2010, 27: A189–A197
5 Aspelmeyer M, Meystre P, Schwab K. Quantum optomechanics. Phys Tod, 2012, 65: 29
6 Wilson-Rae I, Nooshi N, Zwerger W, et al. Theory of ground state cooling of a mechanical oscillator using dynamical backaction. Phys Rev Lett, 2007, 99: 093901
7 Marquardt F, Chen J P, Clerk A A, et al. Quantum theory of cavity-assisted sideband cooling of mechanical motion. Phys Rev Lett, 2007, 99: 093902
8 Vitali D, Gigan S, Ferreira A, et al. Optomechanical entanglement between a movable mirror and a cavity field. Phys Rev Lett, 2007, 98: 030405
9 Phelps G A, Meystre P. Laser phase noise effects on the dynamics of optomechanical resonators. Phys Rev A, 2011, 83: 063838
10 Bhattacharya M, Meystre P. Trapping and cooling a mirror to its quantum mechanical ground state. Phys Rev Lett, 2007, 99: 073601
11 Hartmann M J, Plenio M B. Steady state entanglement in the mechanical vibrations of two dielectric membranes. Phys Rev Lett, 2008, 101: 200503
12 Cheung H K, Law C K. Nonadiabatic optomechanical Hamiltonian of a moving dielectric membrane in a cavity. Phys Rev A, 2011, 84: 023812
13 Thompson J D, Zwickl B M, Jayich A M, et al. Strong dispersive cou-

pling of a high finesse cavity to a micromechanical membrane. Nature, 2008, 452: 72

14 Li Y, Wu L A, Wang Z D. Fast ground-state cooling of mechanical resonators with time-dependent optical cavities. Phys Rev A, 2011, 83: 043804

15 Xu X W, Zhao Y J, Liu Y X. Entangled-state engineering of vibrational modes in a multimembrane optomechanical system. Phys Rev A, 2013, 88: 022325

16 Sun Q, Hu X H, Liu W M, et al. Effect on cavity optomechanics of the interaction between a cavity field and a one-dimensional interacting bosonic gas. Phys Rev A, 2011, 84: 023822

17 Kumar T, Bhattacherjee A B, ManMohan. Dynamics of a movable micromirror in a nonlinear optical cavity. Phys Rev A, 2010, 81: 013835

18 Dalafi A, Naderi M H, Soltanolkotabi M, et al. Nonlinear effects of atomic collisions on the optomechanical properties of a Bose-Einstein condensate in an optical cavity. Phys Rev A, 2013, 87: 013417

19 Zheng Q, Li S C, Zhang X P, et al. Controllable optical bistability of Bose-Einstein condensate in an optical cavity with Kerr medium. Chin Phys B, 2012, 21: 093702

20 Kanamoto R, Meystre P. Optomechanics of a quantum-degenerate Fermi gas. Phys Rev Lett, 2010, 104: 063601

21 Verhagenn E, Deleglise S, Weis S, et al. Quantum-coherent coupling of a mechanical oscillator to an optical cavity mode. Nature, 2012, 482: 63–67

22 Weis S, Rivire R, Delglise S, et al. Optomechanically induced transparency. Science, 2010, 330: 1520–1523

23 Kim K H, Bahl G, Lee W, et al. Cavity optomechanics on a microfluidic resonator with water and viscous liquids. Light Sci Appl, 2013, 2: e110

24 Li Y, Wang Y D, Xue F, et al. Quantum theory of transmission line resonator-assisted cooling of a micromechanical resonator. Phys Rev B, 2008, 78: 134301

25 Xue F, Liu Y X, Sun C P, et al. Two-mode squeezed states and entangled states of two mechanical resonators. Phys Rev B, 2007, 76: 064305

26 Kleckner D, Bouwmeester D. Sub-kelvin optical cooling of a micromechanical resonator. Nature, 2006, 444: 75–78

27 Xia K, Evers J. Ground state cooling of a nanomechanical resonator in the nonresolved regime via quantum interference. Phys Rev Lett, 2009, 103: 227203

28 Liu Y C, Xiao Y F, Luan X, et al. Dynamic dissipative cooling of a mechanical resonator in strong coupling optomechanics. Phys Rev Lett, 2013, 110: 153606

29 Liu Y C, Hu Y W, Wong C W, et al. Review of cavity optomechanical cooling. Chin Phys B, 2013, 22: 114213

30 Wang Y D, Clerk A A. Reservoir-engineered entanglement in optomechanical systems. Phys Rev Lett, 2013, 110: 253601

31 Vitali D, Tombesi P, Woolley M J. Entangling a nanomechanical resonator and a superconducting microwave cavity. Phys Rev A, 2007, 76: 042336

32 Abdi M, Pirandola S, Tombesi P, et al. Entanglement swapping with local certification: Application to remote micromechanical resonators. Phys Rev Lett, 2012, 109: 143601

33 Kuzyk M C, van Enk S J, Wang H. Generating robust optical entanglement in weak-coupling optomechanical systems. Phys Rev A, 2013, 88: 062341

34 Wang C, He L Y, Zhang Y, et al. Complete entanglement analysis on electron spins using quantum dot and microcavity coupled system. Sci China-Phys Mech Astron, 2013, 56: 2054–2058

35 Liu Y M. Virtual-photon-induced entanglement with two nitrogen-vacancy centers coupled to a high-*Q* silica microsphere cavity. Sci China-Phys Mech Astron, 2013, 56: 2138–2142

36 Mancini S, Giovannetti V, Vitali D, et al. Entangling macroscopic oscillators exploiting radiation pressure. Phys Rev Lett, 2002, 88: 120401

37 Pinard M, Dantan A, Vitali D, et al. Entangling movable mirrors in a double-cavity system. Europhys Lett, 2005, 72: 747–753

38 Niedenzu W, Sandner R M, Genes C, et al. Quantum-correlated motion and heralded entanglement of distant optomechanically coupled objects. J Phys B-At Mol Opt Phys, 2012, 45: 245501

39 Dobrindt J M, Wilson-Rae I, Kippenberg T J. Parametric normal-mode splitting in cavity optomechanics. Phys Rev Lett, 2008, 101: 263602

40 Clerk A A, Marquardt F, Jacobs K. Back-action evasion and squeezing of a mechanical resonator using a cavity detector. New J Phys, 2008, 10: 095010

41 Woolley M J, Doherty A C, Milburn G J, et al. Nanomechanical squeezing with detection via a microwave cavity. Phys Rev A, 2008, 78: 062303

42 Safavi-Naeini A H, Groeblacher S, Hill J T, et al. Squeezed light from a silicon micromechanical resonator. Nature, 2013, 500: 185–189

43 Purdy T P, Peterson R W, Regal C. Observation of radiation pressure shot noise on a macroscopic object. Science, 2013, 339: 801–804

44 Ghobadi R, Bahrampour A R, Simon C. Quantum optomechanics in the bistable regime. Phys Rev A, 2011, 84: 033846

45 Marquardt F, Harris J G E, Girvin S M. Dynamical multistability induced by radiation pressure in high-finesse micromechanical optical cavities. Phys Rev Lett, 2006, 96: 103901

46 Fu C B, Yan X B, Gu K H, et al. Steady-state solutions of a hybrid system involving atom-light and optomechanical interactions: Beyond the weak-cavity-field approximation. Phys Rev A, 2013, 87: 053841

47 Agarwal G S, Huang S. Electromagnetically induced transparency in mechanical effects of light. Phys Rev A, 2010, 81: 041803

48 Zhang L, Song Z D. Modification on static responses of a nano-oscillator by quadratic optomechanical couplings. Sci China-Phys Mech Astron, 2014, 57: 880–886

49 Wang H, Sun H C, Zhang J, et al. Transparency and amplification in hybrid system of the mechanical resonator and circuit QED. Sci China-Phys Mech Astron, 2012, 55: 2264–2272

50 Abramovici A, Althouse W E, Drever R W P, et al. LIGO: The laser interferometer gravitational-wave observatory. Science, 1992, 256: 325–333

51 Vitali D, Mancini S, Tombesi P. Optomechanical scheme for the detection of weak impulsive forces. Phys Rev A, 2001, 64: 051401

52 Stannigel K, Rabl P, Sorensen A S, et al. Optomechanical transducers for long-distance quantum communication. Phys Rev Lett, 2010, 105: 220501

53 Liu Y C, Xiao Y F, Chen Y L, et al. Parametric down-conversion and polariton pair generation in optomechanical systems. Phys Rev Lett, 2013, 111: 083601

54 Romero-Isart O, Pflanzer A C, Juan M L, et al. Optically levitating dielectrics in the quantum regime: Theory and protocols. Phys Rev A, 2011, 83: 013803

55 Chang D E, Regal C A, Papp S B, et al. Cavity opto-mechanics using an optically levitated nanosphere. Proc Natl Acad Sci USA, 2010, 107: 1005–1010

56 Pender G A T, Barker P F, Marquardt F, et al. Optomechanical cooling of levitated spheres with doubly resonant fields. Phys Rev A, 2012, 85: 021802

57 Arvanitaki A, Geraci A A. Detecting high-frequency gravitational waves with optically levitated sensors. Phys Rev Lett, 2013, 110: 071105

58 Li T, Kheifets S, Medellin D, et al. Measurement of the instantaneous velocity of a Brownian particle. Science, 2010, 328: 1673–1675

59 Li T, Kheifets S, Raizen M G. Millikelvin cooling of an optically trapped microsphere in vacuum. Nat Phys, 2011, 7: 527–530

60 Yin Z Q. Phase noise and laser-cooling limits of optomechanical oscillators. Phys Rev A, 2009, 80: 033821

61 Yin Z Q, Geraci A A, Li T. Optomechanics of levitated dielectric particles. Int J Mod Phys B, 2013, 27: 1330018
62 Geraci A A, Papp S B, Kitching J. Short-range force detection using optically cooled levitated microspheres. Phys Rev Lett, 2010, 105: 101101
63 Nie W J, Lan Y H, Li Y, et al. Effect of the Casimir force on the entanglement between a levitated nanosphere and cavity modes. Phys Rev A, 2012, 86: 063809
64 Nie W J, Lan Y H, Li Y, et al. Dynamics of a levitated nanosphere by optomechanical coupling and Casimir interaction. Phys Rev A, 2013, 88: 063849
65 Gieseler J, Deutsch B, Quidant R, et al. Subkelvin parametric feedback cooling of a laser-trapped nanoparticle. Phys Rev Lett, 2012, 109: 103603
66 Xuereb A, Paternostro M. Selectable linear or quadratic coupling in an optomechanical system. Phys Rev A, 2013, 87: 023830
67 Romero-Isart O, Juan M L, Quidant R, et al. Toward quantum superposition of living organisms. New J Phys, 201012: 033015
68 Nie W J, Lan Y H, Zhu S Y. Casimir force between topological insulator slabs. Phys Rev B, 2013, 88: 085421
69 Yin Z Q, Li T, Feng M. Three-dimensional cooling and detection of a nanosphere with a single cavity. Phys Rev A, 2011, 83: 013816
70 Romero-Isart Q, Pflanzer A C, Blaser F, et al. Large quantum superpositions and interference of massive nanometer-sized objects. Phys Rev Lett, 2011, 107: 020405
71 Romero-Isart Q. Quantum superposition of massive objects and collapse models. Phys Rev A, 2011, 84: 052121
72 Casimir H B G. On the attraction between two perfectly conducting plates. Proc K Ned Akad Wet Ser B, 1948, 51: 793–795
73 Derjaguin B V, Abrikosova I I, Lifshitz E M. Direct measurement of molecular attraction between solids separated by a narrow gap. Q Rev Chem Soc, 1956, 10: 295–329
74 Bordag M, Mohideen U, Mostepanenko V M. New developments in the Casimir effect. Phys Rep, 2001, 1: 1–205
75 Canaguier-Durand A, Maia Neto P A, Cavero-Pelaez I, et al. Casimir interaction between plane and spherical metallic surfaces. Phys Rev Lett, 2009, 102: 230404
76 Bimonte G, Emig T. Exact results for classical Casimir interactions: Dirichlet and Drude model in the sphere-sphere and sphere-plane geometry. Phys Rev Lett, 2012, 109: 160403
77 Lambrecht A, Reynaud S. Casimir force between metallic mirrors. Eur Phys J D, 2000, 8: 309–318
78 Scardicchio A, Jaffe R L. Casimir effects: An optical approach I. Foundations and examples. Nucl Phys B, 2005, 704: 552–582
79 Butera S, Passante R. Field fluctuations in a one-dimensional cavity with a mobile wall. Phys Rev Lett, 2013, 111: 060403
80 DeJesus E X, Kaufman C. Routh-Hurwitz criterion in the examination of eigenvalues of a system of nonlinear ordinary differential equations. Phys Rev A, 1987, 35: 5288–5290